journal of the mechanical behavior of biomedical materials 147 (2023) 106141

Contents lists available at ScienceDirect

Journal of the Mechanical Behavior of Biomedical Materials

journal homepage: www.elsevier.com/locate/jmbbm

Patient-specific finite element analysis of human corneal lenticules: An experimental and numerical study

Malavika H. Nambiar [a], Layko Liechti [a], Harald Studer [b], Abhijit S. Roy [c], Theo G. Seiler [d,e,f], Philippe Büchler [a,*]

[a] ARTORG Center for Biomedical Engineering Research, University of Bern, Freiburgstrasse 3, 3010, Bern, Switzerland
[b] Optimo Medical, Robert-Walser-Platz 7, 2503, Biel, Switzerland
[c] Narayana Nethralaya Eye Clinic, Bengaluru, Karnataka, 560010, India
[d] IROC AG, Institut für Refraktive und Ophthalmo-Chirurgie, Stockerstrasse 37, 8002, Zürich, Switzerland
[e] Universitätsklinik für Augenheilkunde, Inselspital Bern, Freiburgstrasse 15, 3010, Bern, Switzerland
[f] Klinik für Augenheilkunde, Universitätsklinikum Düsseldorf, Moorenstr. 5, 40225, Düsseldorf, Germany

A B S T R A C T

The number of elective refractive surgeries is constantly increasing due to the drastic increase in myopia prevalence. Since corneal biomechanics are critical to human vision, accurate modeling is essential to improve surgical planning and optimize the results of laser vision correction. In this study, we present a numerical model of the anterior cornea of young patients who are candidates for laser vision correction. Model parameters were determined from uniaxial tests performed on lenticules of patients undergoing refractive surgery by means of lenticule extraction, using patient-specific models of the lenticules. The models also took into account the known orientation of collagen fibers in the tissue, which have an isotropic distribution in the corneal plane, while they are aligned along the corneal curvature and have a low dispersion outside the corneal plane. The model was able to reproduce the experimental data well with only three parameters. These parameters, determined using a realistic fiber distribution, yielded lower values than those reported in the literature. Accurate characterization and modeling of the cornea of young patients is essential to study better refractive surgery for the population undergoing these treatments, to develop in silico models that take corneal biomechanics into account when planning refractive surgery, and to provide a basis for improving visual outcomes in the rapidly growing population undergoing these treatments.

1. Introduction

In the last decades, the prevalence of myopia has drastically increased, with projections of more than half of the world's population being affected by 2050 (Holden et al., 2016). The number of elective refractive surgeries has also dramatically increased (Maller, 2000; McDonnell, 2000; Packer, 2022) at an estimated annual rate of 30% (Packer, 2022), placing a heavy burden on ocular health management services (Holden et al., 2016). The cornea accounts for 2/3 of the refractive power of the eye making its shape the most important determinant of ocular refraction. Corneal curvature is determined by the biomechanical properties of the cornea and is a response to intraocular pressure. Therefore, any surgical intervention that affects the corneal stiffness and tension modifies its shape, and consequently the patient's refractive power and vision. Accurate quantification of these biomechanical properties is therefore necessary to estimate the outcome of refractive procedures.

Most patients undergoing refractive surgery are under 33 years of age (Mohammadi et al., 2018), but much of the current knowledge about the mechanical behavior of human corneas comes from porcine studies (Elsheikh, A. et al., 2008; Elsheikh and Alhasso, 2009). However, human corneas differ physiologically from porcine corneas, such that human tissue has two orthogonal bundles of collagen fibers in the center that radially transition to a circumferential orientation, in contrast to the purely circumferential arrangement of the single bundle collagen arrangement in porcine corneas (Hayes et al., 2007). Due to the difficulties in obtaining human samples, there are only a few studies characterizing human corneas (Elsheikh et al., 2005; Kanellopoulos, 2018; Randleman et al., 2008a; Whitford et al., 2015), mainly from donors older than 50 (Arya et al., 2021; "EBAA Eye banking statistical report 2019," 2020). Since corneal biomechanics changes with age as it stiffens due to non-enzymatic cross-linking that occurs over time (Elsheikh et al., 2007), the characterization of young human corneal tissue is essential to plan refractive interventions such as photorefractive keratectomy (PRK),

* Corresponding author.
E-mail addresses: malavika.nambiar@unibe.ch (M.H. Nambiar), liechti.layko@gmail.com (L. Liechti), harald.studer@optimo-medical.com (H. Studer), asroy27@yahoo.com (A.S. Roy), theo@seiler.tv (T.G. Seiler), philippe.buechler@unibe.ch (P. Büchler).

https://doi.org/10.1016/j.jmbbm.2023.106141
Received 16 February 2023; Received in revised form 5 May 2023; Accepted 20 September 2023
Available online 21 September 2023

laser-assisted in situ keratomileusis (LASIK) and lenticule extraction in young people.

Lenticule extraction surgeries such as CLEAR, SMILE, and Smartsight represent a source of young cornea samples (Fuest and Mehta, 2021). In these procedures, a femtosecond laser is used to excise a lens-shaped element called lenticule from the patient's stroma, and small incisions are made to remove this tissue, reshaping the cornea and correcting the patient's vision. The lenticule removed during the procedure is usually discarded but can be used for mechanical characterization. This approach has been used by the Wang group (Liu et al., 2020; Song et al., 2022; Xiang et al., 2018; Xue et al., 2018, 2021) to mechanically test stromal strips extracted from the lenticules. The authors were able to show that the mechanical response was similar between the nasal-temporal (NT) and superior-inferior (SI) testing directions and identify the parameters of a non-linear mechanical model (Liu et al., 2020). However, the mechanical testing method used in these studies employed rigid clamps as holders and very small sample dimensions (~1 mm × 1.5 mm), which questions the homogeneity of the stress and strain in the tested specimens.

In addition, the material identification based on the tested lenticules was performed assuming ideal uniaxial elongation, which is only an approximation of the constantly changing thickness of the lenticule and non-uniform deformation of the sample during testing. These limitations may lead to an inaccurate estimate of the material response (Sun et al., 2005). Furthermore, the parameter identification derived from these lenticule studies considered a preferential alignment of the collagen fibers in the NT and SI directions, while it is known that the anterior part of the cornea has an isotropic in-plane distribution of the collagen fibers, and only shows little out-of-plane dispersion (Abass et al., 2015; Andrew J. Quantock et al., 2007; Winkler et al., 2013a).

Therefore, the objective of this study is to determine the parameters of an anisotropic and hyperelastic material model based on the known distribution of collagen fibers of the anterior cornea, taking into account the shape of each lenticule and the load on each sample. We have also mechanically characterized human corneal lenticules by performing uniaxial tests that rely on a large aspect ratio between the length and width of the samples and a hook attachment system to better approximate the uniaxial situation.

2. Methods

2.1. Experimental measurements

Five human corneal lenticules from four patients in the age group 27–30 were included in this study (KEK approval 2021–00145). The patients underwent CLEAR surgery (Ziemer Ophthalmic Systems AG, Switzerland) for optical corrections of −3.25 to −4.5 D, with little to no astigmatism (<1 D). Tissue samples were collected after surgery and were uniaxially tested within 24 h after the intervention. The lenticules had a diameter between 6.8 mm and 7 mm and had a nonconstant thickness that varied depending on the specific refractive correction of the patient (Table 1). Both corneal tomography and cutting profile were recorded for each patient.

The samples were individually preserved and tested uniaxially in a hydration-preserving corneal culture media containing 5% Dextran.

Table 1
Surgical parameters for the respective samples used to generate the geometry for each sample.

	S1	S2	S3	S4	S5
Age (y)	29	27	29	30	30
Cap Thickness [mm]	130	115	130	115	115
Surgical diameter [mm]	7.0	6.8	7.0	6.8	6.8
Corrected Sphere [D]	−3.75	−3.50	−3.25	−4.50	−3.75
Corrected Cylinder [D]	−0.25	−0.75	−0.75	0	0
Axis [deg]	180°	60°	8°	180°	180°

Mechanical testing was conducted using the UStretch device (CellScale, Waterloo, Canada) with BioRake attachments (3 tines, 0.25 mm diameter) at room temperature (Fig. 1). The tissue was pre-stretched to 10 mN to ensure the tautness of the tissue and device. The samples were preconditioned with five cycles of 10% strain at a loading speed of 0.007 mm/s. The last cycle of force-displacement data was recorded for analysis.

2.2. Finite element mesh

Preoperative corneal topography data were obtained for all five patients. A surface mesh representing the anterior corneal surface was created from the elevation profile given by Pentacam measurements (Oculus, Arlington, USA). The epithelium was assumed to have a constant thickness of 50 μm. The surgical parameters such as the cap thickness, plane parallel layer, and the patient's spherical and cylindrical correction were taken from the surgical planning to derive the laser cutting profile using the Mrochen formula (Mrochen et al., 2004), which accounts for higher order aberrations. Since the extracted lenticles have a non-constant thickness, inverse finite element simulations based on the patient-specific geometry of the lenticles were used to determine the material parameters. The finite element mesh of the lenticule was then reconstructed from these two surfaces using the open-source Python library GMSH (Geuzaine and Remacle, 2009). The code for generating and meshing lenticules from the Pentacam clinical dataset and surgical parameters is freely available at: https://github.com/Malavika-94/FEM-generation-of-a-patient-specific-lenticule-based-on-Pentacam-Data.

In addition to the patient-specific lenticule geometry, the finite element model had the same boundary conditions as the experimental setup. The hook attachment points were modeled as three holes with a diameter of 0.25 mm and a distance of 0.7 mm between their centers. The boundary conditions were applied to the attachment holes; the model was fixed on one side while the displacement recorded experimentally was imposed on the opposite side. Note that only the displacement in the direction of traction was imposed on the model, allowing the distance between the holes to change according to the mechanical loading (Fig. 2). The models were meshed with approximately 8000 s-order tetrahedral elements.

2.3. Material model

The strain-energy function considered the dispersed collagen fibers using a weighted integration of the Holzapfel Gasser Ogden (HGO) (Gasser et al., 2006) model over the unit sphere (Volokh, 2017):

$$U = C_{10}(\bar{I}_1 - 3) + \int_0^{\pi}\int_0^{2\pi} \rho(\boldsymbol{a})\left\{\frac{k_1}{2k_2}\left\{\exp\left[k_2 <\bar{E}>^2\right] - 1\right\}\right\}\sin\theta\, d\theta d\varphi$$

$$\bar{E} = \bar{I}_4(\mathbf{a}) - 1$$

where C_{10}, k_1, and k_2, are material parameters, $\boldsymbol{a}$ is the generic fiber direction is spherical coordinates

$$\mathbf{a}(\varphi,\theta) = \cos\varphi\sin\theta\,\boldsymbol{e}_1 + \sin\varphi\sin\theta\,\boldsymbol{e}_2 + \cos\theta\boldsymbol{e}_3$$

$$0 \le \varphi \le 2\pi, 0 \le \theta \le \pi$$

$\bar{I}_1$ and $\bar{I}_4$ are invariants of the isochoric Cauchy-Green strain tensor $\overline{\mathbf{C}} = \boldsymbol{J}^{2/3}\mathbf{F}^T\mathbf{F}$, $\mathbf{F}$ is the deformation gradient tensor, and $J = det\,\mathbf{F}$. The operator $<\bullet>$ represents the Macauley bracket, which accounts for the fact that collagen fibers contribute only when they are under tension:

$$\bar{I}_1 = Tr\,\overline{\mathbf{C}}$$

$$\bar{I}_4 = (\mathbf{a}\otimes\mathbf{a}) : \overline{\mathbf{C}}$$

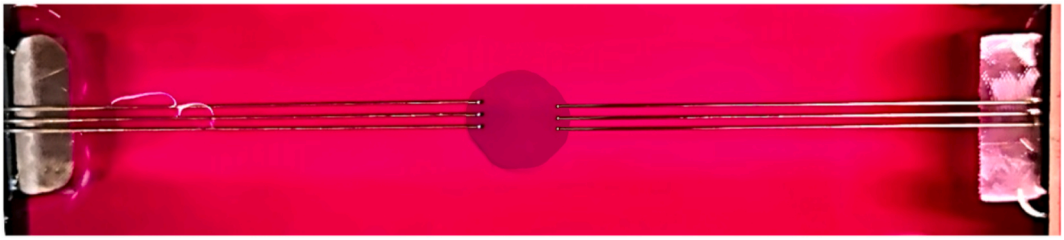

Fig. 1. The lenticule was tested under traction in a bath of MEM + 5% Dextran using BioRake attachments.

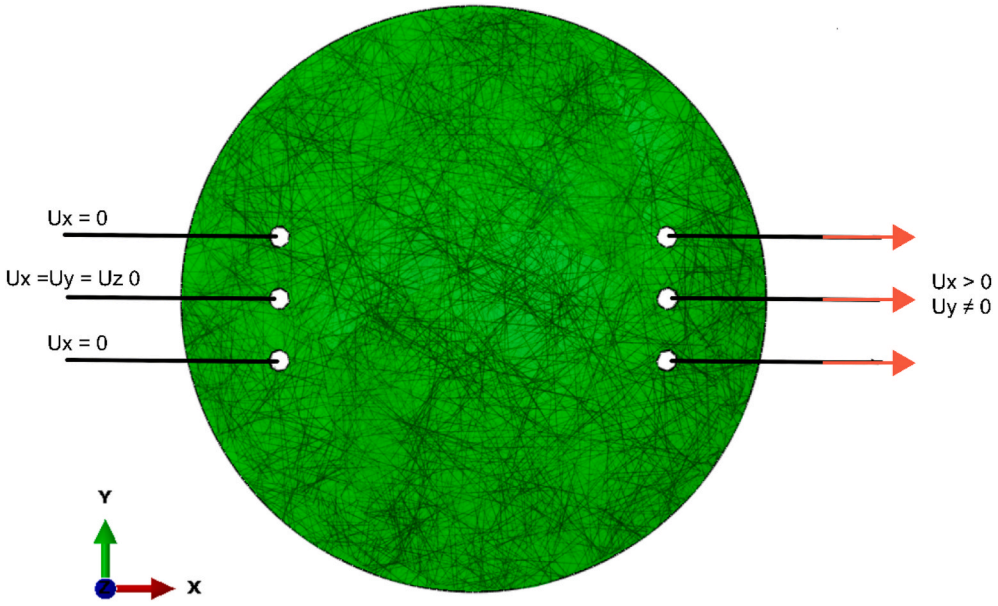

Fig. 2. Finite element model and the boundary conditions applied to the lenticule model to determine its mechanical properties.

$$< \overline{E} > = \begin{cases} \overline{E} & \overline{E} > 0 \\ 0 & \overline{E} \leq 0 \end{cases}$$

and ρ is the is the angular density of the fiber distribution decomposed as a product of the in-plane $\rho_{ip}(\varphi)$ and out-of-plane distributions $\rho_{op}(\theta)$:

$$\rho(\varphi, \theta) = \rho_{op}(\theta)\rho_{ip}(\varphi)$$

$$\rho_{op}(\theta) = 2\sqrt{\frac{2b}{\pi}} \frac{\exp[-2b\, cos^2\, \theta]}{\mathrm{erf}(\sqrt{2b})} \quad , 0 \leq \theta \leq \pi$$

$$\rho_{ip}(\varphi) = \frac{\exp[a \cos 2\, \varphi]}{I_0(a)} \quad , 0 \leq \varphi \leq 2\pi$$

a and b are the material constants defined as $a = 0$ and $b = 2.5$ based on X-ray diffraction data (Abass et al., 2015) indicating an isotropic dispersion in the plane and aligned distribution out of plane (Fig. 3). I_0 is the modified Bessel function of the first kind of order 0.

Numerically, the integration over the unit sphere of the material model is discretized using the Lebedev quadrature scheme (Lebedev, 1977). A parametric evaluation revealed a difference of less than 0.009% between the full Lebedev scheme with 5180 integrations and that with 350 integrations. Therefore, in the interest of computational time, the discretization was set to 350 fibers for all calculations. The finite element simulations were performed using Abaqus (Dassault Systemes Simulia Corp, 2020), and the material was implemented using a user subroutine.

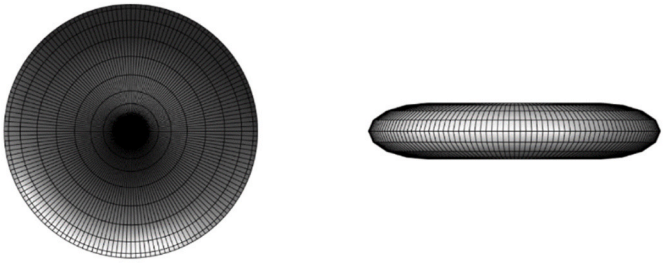

Fig. 3. The corneal in-plane (a = 0) and out of plane (b = 2.5) dispersion of the fibers.

2.4. Parameter identification

A Bayesian optimization was used to identify the material parameters based on the experimental data (bayesian-optimization)(Nogueira, 2014). Patient-specific material parameters were determined for each sample individually, and a general optimization was performed to determine the parameters that best matched the experimental response of all samples simultaneously. In this case, the loss function was calculated as the average root mean squared distance between the numerical and experimental data of all samples, which required simulation of the five samples for each iteration of the optimizer.

The solution with the lowest loss was chosen as the best-fit parameter for the general model. For the patient-specific models, a regularization

technique was used to avoid local minimas in the selection of the solution. Therefore, the parameters that resulted in a loss that was less than 10% from the absolute minima were selected. From these local minima, the parameters that were closest to the parameters of the general model were selected as the optimal solution for the individualized models.

3. Results

Twelve samples were obtained from the clinic from six patients based on the inclusion criteria. Five samples from four patients were included in the analysis. The collected samples showed no signs of damage after surgical extraction. The main reason for exclusion was damage to the samples at the attachment points during the mechanical testing. The force-displacement response during uniaxial loading was measured for each sample and showed a typical non-linear behavior (Fig. 4). The five cycles of preconditioning are shown in Fig. 4 (a). The first cycle exhibits the highest hysteresis, followed by subsequent reductions in maximum force, stabilizing by the 5th cycle which was used in the numerical analysis (Fig. 4, b).

The experimental arrangement is capable of effectively stressing the corneal tissue located between the hook attachments. However, the volume of stressed tissue decreases with distance from the attachment, being less in the central area than near the attachment. During testing, the amount of stress was also lower in the central region of the specimens and increased with proximity to the attachments. As expected, the high stresses are concentrated in the tissue near the hook attachments, where the failure occurred experimentally (Fig. 5).

Optimization of the mechanical parameters resulted in a good agreement with the experimental data for the general and the patient-specific models (Fig. 6). The patient-specific model produced an almost perfect match with the experimental data, with a loss of less than 25 mN (Table 2). While the parameters of the model obtained simultaneously for all samples resulted in a higher loss (94 mN), this general model provided a good estimate of the force-displacement behavior of all specimens. In addition, the parameters of the general model are close to the mean of the individual identification, and well within the SD of the individually fitted models.

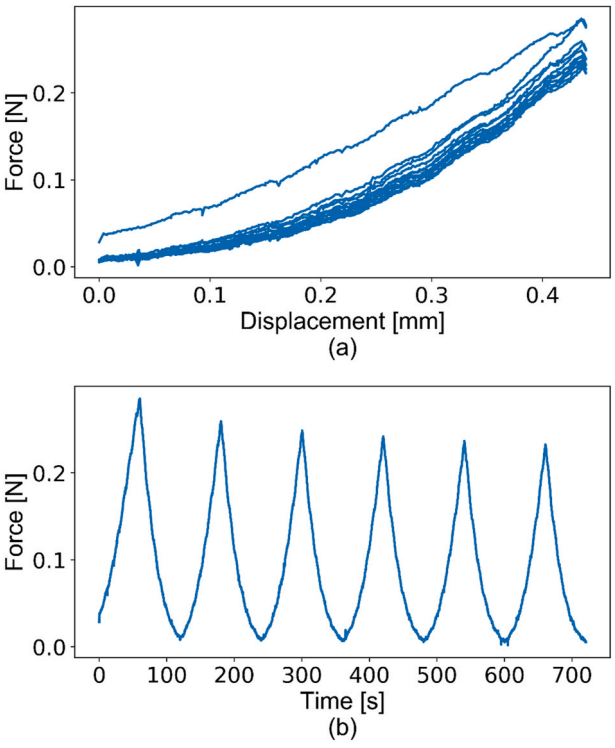

Fig. 4. (a) A typical force-displacement graph of 6 cycles for preconditioning. The first curve shows a significant hysteresis loop, typical for a viscoelastic material. (b) The force-time graph shows the drop in the magnitude of force which stabilizes between the 5th -6th cycle.

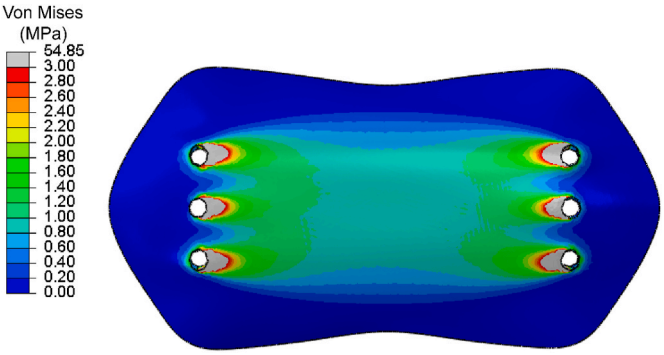

Fig. 5. Von Mises stress distribution of a lenticule model under 10% strain. The stress patterns are uniform in the central region and increase closer to the attachments. The highest stresses are observed at the attachments.

A comparison between one of the patient-specific models fitted with general parameters within the experimental force-displacement range of all patients is shown in Fig. 7. Overall, the results of the study showed that the mechanical behavior of the human cornea could be accurately captured using a patient-specific finite element model, with good agreement between the numerical simulations and the experimental data.

4. Discussion

The aim of this study was to propose a numerical model of the anterior cornea of young patients based on the known distribution of collagen fibers. First, the biomechanical behavior of the lenticule obtained after refractive surgery was quantified using uniaxial tensile tests. Second, the parameters of a Holzapfel-Gasser-Ogden material model were determined using a numerical model based on patient-specific geometry. This material model accounts for different fiber dispersions in the corneal plane and transverse to it. We present a method for determining the patient-specific properties of human lenticules and an accurate mechanical description of the young anterior cornea.

Although the characterization of the anterior stroma was performed using tensile tests by the Wang group (Liu et al., 2020; Song et al., 2022; Xiang et al., 2018; Xue et al., 2018, 2021), this study proposes improvements in both the experimental design and the determination of the model parameters. Regarding the experimental design, in the published studies, lenticule strips of approximately equal length and width were prepared and rigidly clamped at both ends, leaving only a distance of 1.5 mm of the sample to be tested. Moreover, these samples were tested in media not designed to maintain hydration (Liu et al., 2020; Song et al., 2022; Xue et al., 2018), which compromises the characterization (Sun et al., 2005; Xia et al., 2014). In this study, we proposed using a hook attachment system instead of rigid clamps and long specimens that are approximately three times as long as they are wide. This allows for lateral contraction in the direction orthogonal to the tensile force and thus a better distribution of the force applied to the specimen, resulting in a load that is closer to a uniaxial test. The tests were also performed in a medium that preserves hydration and prevents swelling. In addition, the lenticules in this study were not further cut into strips but tested directly; this prevents damage to the tissue from manual cutting and preserves the natural fiber reinforcement of the specimens by collagen.

Despite these differences in experimental design, the stress-strain relationship derived from the present study is within the range of previously published data. However, the shape of the nonlinear relationship

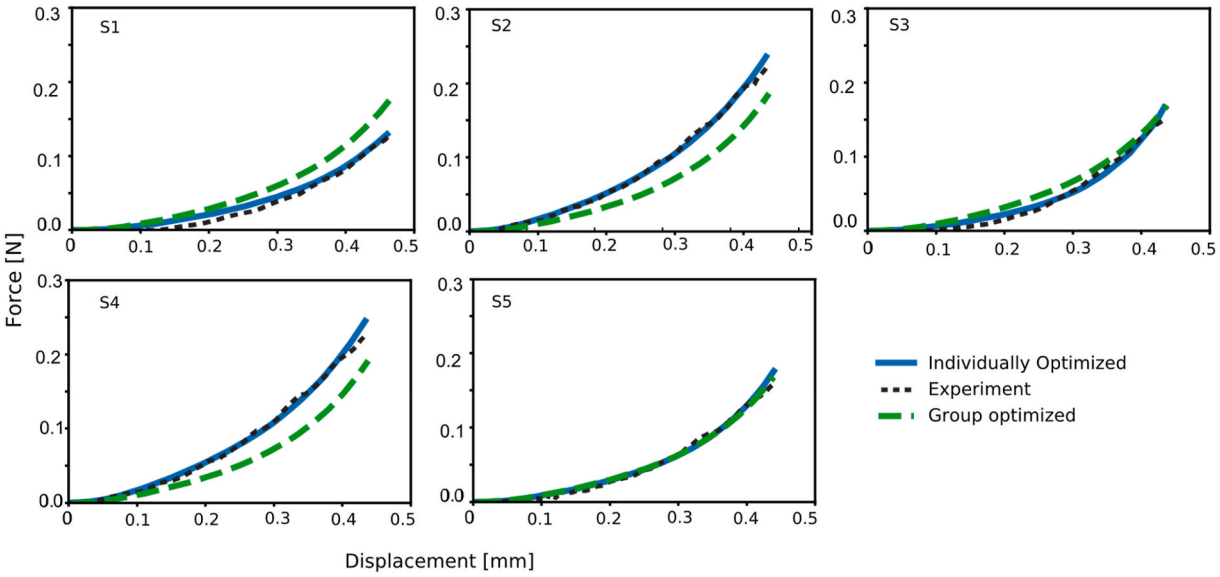

Fig. 6. Force-displacement relationship for each sample, computed experimentally and numerically in an individually optimised way and as simultaneous fitting on the whole group.

Table 2
Parameters of the individual models (S1–S5) and the general fitting model.

	S1	S2	S3	S4	S5	Mean	SD	General
C10 (kPa)	20	21	24	10	24	20	5.7	24.05
k1 (MPa)	3.3	24.4	4.2	11.1	7.1	7.5	3.8	4.98
k2	51.96	18.31	47.91	19.06	27.69	32.99	15.97	40.34
Loss (N)	0.034	0.018	0.035	0.017	0.02	0.025	0.009	0.094

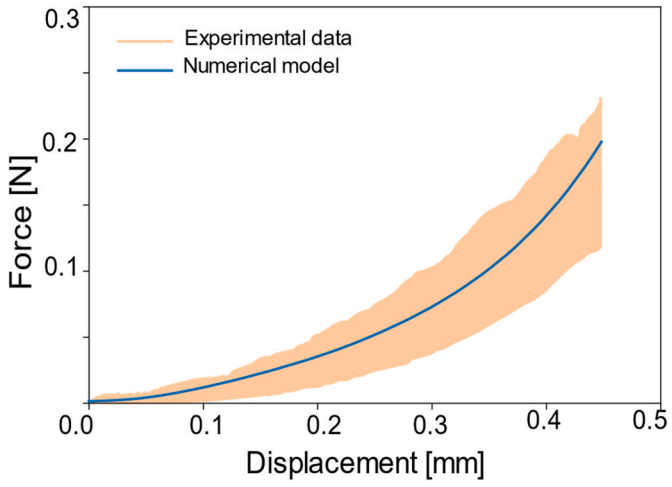

Fig. 7. A general model represented the range of experimental force-displacement data obtained in this study.

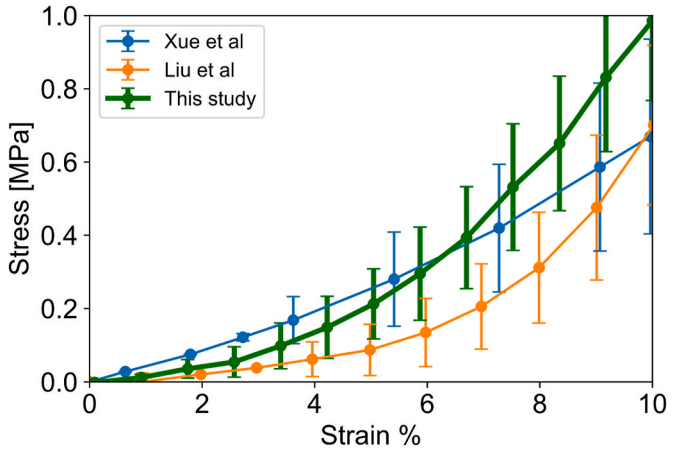

Fig. 8. Stress-strain comparison of literature data represented as a mean and standard deviation to this study.

differs, with the present study reporting stiffer properties for strains above 6% (Fig. 8). This difference could be attributed to the different test method; a non-hydration preserving solution may cause the sample to swell and therefore decrease the calculated stress for the same measured force. This difference may also be due to the different definitions of the reference position from which the force and displacements are measured, which directly affects the strain calculation and may cause a shift in the overall stress-strain curve. Interestingly, the force-displacement data obtained in this study are similar to those reported for porcine anterior corneal strips of similar thickness (Nambiar et al., 2022). Despite the different morphologic orientation of collagen between porcine and human corneas as demonstrated by X-ray scattering (Hayes et al., 2007), the anterior part of the cornea shows a similar isotropic distribution of fibers, whereas the morphological differences occur in the layers of the tissue. Although Nambiar et al. used a circumferential orientation through the cornea, the dispersion parameters determined in the anterior part of the cornea indicate isotropy. This suggests that the anterior part of the human and porcine corneas exhibit similar behavior and that it is important to consider isotropic fiber distribution when modeling this part of the cornea.

To our knowledge, this is the first study to reproduce the patient-specific geometry of the lenticule based on surgical data and to

estimate the material parameters. Most numerical characterizations in the literature refer to material estimates of the entire cornea (Ariza--Gracia et al., 2017; Pandolfi and Manganiello, 2006; Sinha Roy et al., 2014; Studer et al., 2010). These do not capture the depth-dependent biomechanics or microstructure of the cornea (Randleman et al., 2008b). The ones that do (Wang and Hatami-Marbini, 2021; Winkler et al., 2013a), also rely on experimental data obtained from aged donor corneas from eye banks or porcine eyes. It is well known that aged corneas have different material properties than young corneas (Elsheikh et al., 2007). Therefore, experimental and numerical characterization of young corneas is needed to develop in silico models for refractive surgery for the population receiving these treatments.

For the characterization of the anterior segment, only one study by Liu et al. uses the finite element method to model the strip experiments. However, in this study, the FE simulation corresponds to a pure uniaxial setup rather than an accurate representation of the experiments. The motivation for using the FE model was not to capture the exact geometry of the sample or its deformation during testing, but to implement an advanced material model to capture the crimping effect of collagen fibers based on observations from transmission electron microscopy and to better represent the biomechanics of the tissue in the physiological 'toe' region. However, this model assumes that collagen fibers have two preferred perpendicular orientations in the naso-temporal and superior-inferior directions. While this distribution has been demonstrated for the entire cornea, its anterior segment exhibits an isotropic fiber distribution; high-resolution microscopy and small-angle X-ray scattering studies have shown that healthy anterior corneas do not have a preferential orientation in the corneal plane and are aligned parallel to the corneal plane (Andrew J Quantock et al., 2007; Winkler et al., 2013b). This dispersion is also clearly depth-dependent, with preferential in the plane alignment visible in the posterior cornea (Abass et al., 2015; Andrew J. Quantock et al., 2007; Winkler et al., 2013b). In this study, this asymmetric dispersion of collagen fibers is captured by an in-plane isotropic probability density function ($a = 0$) and an out-of-plane aligned fiber distribution ($b = 2.5$).

From a numerical point of view, the angular integration of a large number of discrete fibers - 350 in this study - required at each increment for all integration points represents a significant computational cost. The general structure tensor (GST) has been proposed to alleviate this problem by incorporating the fiber distribution directly into a reformulated invariant of the constitutive model (Gasser et al., 2015; Holzapfel et al., 2000). However, this GST approach does not appear to be suitable for modeling the uniaxial experiment of the anterior cornea, which has an isotropic distribution of fiber orientation in the plane. First, the GST approach is not able to deactivate collagen fibers that are in compression, which is the case for fibers perpendicular to the loading direction in the uniaxial test. Second, the GST approach has been shown to provide accurate stresses only when dispersion is low and fibers are predominantly aligned in the main fiber direction. However, when dispersion is large, as is the case with the anterior stroma, the accuracy of the approach can significantly underestimate stresses with an error of up to 100% at 10% strain (Melnik et al., 2015), likely leading to an overestimation of material properties (Pandolfi and Holzapfel, 2008). Modified versions of the GST have been proposed without completely eliminating these problems (Melnik et al., 2015; Pandolfi and Vasta, 2012). For these reasons, the angular integration method is used in this study, which allows accurate stress calculations despite the longer calculation times required.

The main limitation of this study is the small number of samples. However, the patients included in this study are a homogeneous group with similar ages and similar refractive corrections in both sphere and cylinder. Therefore, we were able to propose general model parameters that provide a robust estimation of the mechanical properties of this population based on all the collected samples. The fact that this general model reproduces the individual cases well, confirms that it is a good description of this target population of young corneas requiring moderate refractive correction. Another limitation is the uniaxial test used, which does not correspond to the physiological multidirectional loading conditions that exists in the cornea. Alternative methods have been proposed to better reproduce these conditions, such as corneal inflation or biaxial testing (Elsheikh et al., 2005; Kanellopoulos, 2018). Nevertheless, uniaxial testing remains a popular method for characterizing the mechanical behavior of materials because of its ease of use and to analyze, especially for small and transparent specimens such as human lenticules. When used in conjunction with numerical parameter identification, it can also provide a good estimate of the mechanical behavior of the cornea.

An anisotropic material model was used in the study, although lenticles from the anterior part of the cornea have an isotropic fiber distribution in the test plane. The anisotropic model used in this work is not only able to account for the out-of-plane orientation of fibers, but can also be applied to the entire cornea so that the isotropic distribution in the anterior part of the cornea can be transformed to account for the specific in-plane and out-of-plane orientations found experimentally. For example, fibers in the central cornea transition from an isotropic orientation in the anterior part of the cornea to a more vertical and horizontal orientation as they move toward the posterior part of the cornea.

The attachment of the rakes to the sample has been approximated by displacement boundary conditions in the finite element model. The approximation does not capture the deformation of the attachment holes under the load applied to the holes by the rakes during testing. This approximation does have a small effect on the stress distribution around the attachment, but this effect is local to the stress around the rakes and does not affect the total stress calculated in the specimen or the total force calculated in the rakes.

In the study, a mechanical model of the biomechanics of the human anterior stroma was proposed in young patients aged about 30 years and with a refractive correction of about 4D. Special care was taken to include patient-specific geometry and morphological fiber dispersion in the numerical model of the lenticule to determine material properties from experimental measurements. The proposed approach is general and can be extended to allow individual mechanical characterization of specific patients or to include the biomechanics of the central and posterior stroma so that a model of the entire cornea can be created. Accurate characterization and modelling of the cornea of young patients is essential to better study refractive surgery for the population undergoing these treatments, to develop in silico models that take corneal biomechanics into account when planning refractive surgery, and to provide a basis for improving visual outcomes in the rapidly growing population undergoing these treatments.

Code availability

The code for generating and meshing lenticules from the Pentacam clinical dataset and surgical parameters is freely available at: https://github.com/Malavika-94/FEM-generation-of-a-patient-specific-lenticule-based-on-Pentacam-Data.

CRediT authorship contribution statement

Malavika H. Nambiar: Writing – review & editing, Writing – original draft, Validation, Methodology, Formal analysis, Data curation, Conceptualization. **Layko Liechti:** Validation, Methodology, Investigation, Formal analysis, Data curation. **Harald Studer:** Project administration, Methodology, Funding acquisition. **Abhijit S. Roy:** Project administration, Methodology, Funding acquisition. **Theo G. Seiler:** Writing – review & editing, Supervision, Investigation, Data curation. **Philippe Büchler:** Writing – review & editing, Supervision, Methodology, Funding acquisition, Formal analysis, Conceptualization.

Declaration of competing interest

The authors declare that they have no known competing financial interests or personal relationships that could have appeared to influence the work reported in this paper.

Data availability

Data will be made available on request.

Acknowledgment

This study was funded by the Swiss National Science Foundation, Switzerland (IZLIZ3_182975). The authors thank the participants of this study and Ms. Inza Naqvi for her contribution to the figures. There are no conflicts of interests.

References

Abass, A., Hayes, S., White, N., Sorensen, T., Meek, K.M., 2015. Transverse depth-dependent changes in corneal collagen lamellar orientation and distribution. J. R. Soc. Interface 12. https://doi.org/10.1098/rsif.2014.0717.

Ariza-Gracia, M., Ortillés, Cristóbal, J., Rodríguez Matas, J.F., Calvo, B., 2017. A numerical-experimental protocol to characterize corneal tissue with an application to predict astigmatic keratotomy surgery. J. Mech. Behav. Biomed. Mater. 74, 304–314. https://doi.org/10.1016/j.jmbbm.2017.06.017.

Arya, S.K., Raj, A., Deswal, J., Kohli, P., Rai, R., 2021. Donor demographics and factors affecting corneal utilisation in Eye Bank of North India. Int. Ophthalmol. 41, 1773–1781. https://doi.org/10.1007/s10792-021-01736-x.

EBAA Eye banking statistical report 2019, 2020. Eye Bank Assoc Am, pp. 1–110.

Elsheikh, A., Brown, M., Alhasso, D., Rama, P., Campanelli, M., Garway-Heath, D., 2008. Experimental assessment of corneal anisotropy. J. Refract. Surg. Off. Publ. Int. Soc. Refract. Surg. 24.

Elsheikh, A., Alhasso, D., 2009. Mechanical anisotropy of porcine cornea and correlation with stromal microstructure. Exp. Eye Res. 88, 1084–1091. https://doi.org/10.1016/j.exer.2009.01.010.

Elsheikh, A., Anderson, K., Interface, J.R.S., Elsheikh, A., Anderson, K., 2005. Comparative Study of Corneal Strip Extensometry and Inflation Tests Comparative Study of Corneal Strip Extensometry and Inflation Tests 177–185. https://doi.org/10.1098/rsif.2005.0034.

Elsheikh, A., Wang, D., Brown, M., Rama, P., Campanelli, M., Pye, D., 2007. Assessment of corneal biomechanical properties and their variation with age. Curr. Eye Res. 32, 11–19. https://doi.org/10.1080/02713680601077145.

Fuest, M., Mehta, J., 2021. Advances in refractive corneal lenticule extraction. Taiwan J. Ophthalmol. 11, 113. https://doi.org/10.4103/tjo.tjo_12_21.

Gasser, T.C., Ogden, R.W., Holzapfel, G.A., 2015. Modelling non-symmetric collagen fibre dispersion in arterial walls. J. R. Soc. Interface 3, 15–35. https://doi.org/10.1098/rsif.2005.0073.

Gasser, T.C., Ogden, R.W., Holzapfel, G.A., 2006. Hyperelastic modelling of arterial layers with distributed collagen fibre orientations. J. R. Soc. Interface 3, 15–35. https://doi.org/10.1098/rsif.2005.0073.

Geuzaine, C., Remacle, J.-F., 2009. Gmsh: a Three-Dimensional Finite Element Mesh Generator with Built-In Pre- and Post-processing Facilities.

Hayes, S., Boote, C., Lewis, J., Sheppard, J., Abahussin, M., Quantock, A.J., Purslow, C., Votruba, M., Meek, K.M., 2007. Comparative study of fibrillar collagen arrangement in the corneas of primates and other mammals. Anat. Rec. 290, 1542–1550. https://doi.org/10.1002/ar.20613.

Holden, B.A., Fricke, T.R., Wilson, D.A., Jong, M., Naidoo, K.S., Sankaridurg, P., Wong, T.Y., Naduvilath, T.J., Resnikoff, S., 2016. Global prevalence of myopia and high myopia and temporal trends from 2000 through 2050. Ophthalmology. https://doi.org/10.1016/j.ophtha.2016.01.006.

Holzapfel, G.A., Gasser, T.C., Ogden, R.A.Y.W., 2000. A New Constitutive Framework for Arterial Wall Mechanics and a Comparative Study of Material Models, pp. 1–48.

Kanellopoulos, A.J., 2018. Comparison of corneal biomechanics after myopic small-incision lenticule extraction compared to lasik: an ex vivo study. Clin. Ophthalmol. 12, 237–245. https://doi.org/10.2147/OPTH.S153509.

Lebedev, V.I., 1977. Spherical quadrature formulas exact to orders 25-29. Sib. Math. J. 18, 99–107. https://doi.org/10.1007/BF00966954/METRICS.

Liu, T., Shen, M., Huang, L., Xiang, Y., Li, H., Zhang, Y., Wang, Y., 2020. Characterization of hyperelastic mechanical properties for youth corneal anterior central stroma based on collagen fibril crimping constitutive model. J. Mech. Behav. Biomed. Mater. 103, 103575 https://doi.org/10.1016/j.jmbbm.2019.103575.

Maller, B.S., 2000. Market trends in refractive surgery. Int. Ophthalmol. Clin. 40, 11–19. https://doi.org/10.1097/00004397-200007000-00004.

McDonnell, P.J., 2000. Emergence of refractive surgery. Arch. Ophthalmol. 118, 1119–1120. https://doi.org/10.1001/archopht.118.8.1119.

Melnik, A.V., Borja Da Rocha, H., Goriely, A., 2015. On the modeling of fiber dispersion in fiber-reinforced elastic materials. Int. J. Non. Linear. Mech. 75, 92–106. https://doi.org/10.1016/j.ijnonlinmec.2014.10.006.

Mohammadi, S.F., Alinia, C., Tavakkoli, M., Lashay, A., Chams, H., 2018. Refractive surgery: the most cost-saving technique in refractive errors correction. Int. J. Ophthalmol. 11, 1013–1019. https://doi.org/10.18240/ijo.2018.06.20.

Mrochen, M., Donitzky, C., Wüllner, C., Löffler, J., 2004. Wavefront-optimized ablation profiles: theoretical background. J. Cataract Refract. Surg. https://doi.org/10.1016/j.jcrs.2004.01.026.

Nambiar, M.H., Liechti, L., Müller, F., Bernau, W., Studer, H., Roy, A.S., Seiler, T.G., Büchler, P., 2022. Orientation and depth dependent mechanical properties of the porcine cornea: experiments and parameter identification. Exp. Eye Res. 224, 109266 https://doi.org/10.1016/j.exer.2022.109266.

Nogueira, F., 2014. Bayesian Optimization:Open Source Constrained Global Optimization Tool for Python [WWW Document]. 2014–. URL. https://github.com/fmfn/BayesianOptimization.

Packer, M., 2022. Refractive surgery current status: expanding options. Expet Rev. Ophthalmol. 17, 231–232. https://doi.org/10.1080/17469899.2022.2108405.

Pandolfi, A., Holzapfel, G.A., 2008. Three-dimensional modeling and computational analysis of the human cornea considering distributed collagen fibril orientations. J. Biomech. Eng. 130 https://doi.org/10.1115/1.2982251.

Pandolfi, A., Manganiello, F., 2006. A model for the human cornea: constitutive formulation and numerical analysis. Biomech. Model. Mechanobiol. 5, 237–246. https://doi.org/10.1007/s10237-005-0014-x.

Pandolfi, A., Vasta, M., 2012. Fiber distributed hyperelastic modeling of biological tissues. Mech. Mater. 44, 151–162. https://doi.org/10.1016/j.mechmat.2011.06.004.

Quantock, Andrew J., Boote, C., Young, R.D., Hayes, S., 2007a. Small-angle Fibre Diffraction Studies of Corneal Matrix Structure : a Depth-Profiled Investigation of the Human Eye-Bank Cornea, pp. 335–340. https://doi.org/10.1107/S0021889807005523.

Quantock, Andrew J., Boote, C., Young, R.D., Hayes, S., Tanioka, H., Kawasaki, S., Ohta, N., Iida, T., Yagi, N., Kinoshita, S., Meek, K.M., 2007b. Small-angle fibre diffraction studies of corneal matrix structure: a depth-profiled investigation of the human eye-bank cornea. J. Appl. Crystallogr. 40, 335–340. https://doi.org/10.1107/S0021889807005523.

Randleman, J.B., Dawson, D.G., Grossniklaus, H.E., McCarey, B.E., Edelhauser, H.F., 2008a. Depth-dependent cohesive tensile strength in human donor corneas: implications for refractive surgery. J. Refract. Surg. 24 https://doi.org/10.3928/1081597x-20080101-15.

Randleman, J.B., Dawson, D.G., Grossniklaus, H.E., McCarey, B.E., Edelhauser, H.F., 2008b. Depth-dependent cohesive tensile strength in human donor corneas: implications for refractive surgery. J. Refract. Surg. 24, 20080101 https://doi.org/10.3928/1081597x-20080101-15.

Sinha Roy, A., Dupps, W.J., Roberts, C.J., 2014. Comparison of biomechanical effects of small-incision lenticule extraction and laser in situ keratomileusis: finite-element analysis. J. Cataract Refract. Surg. 40, 971–980. https://doi.org/10.1016/j.jcrs.2013.08.065.

Song, Y., Wu, D., Shen, M., Wang, L., Wang, C., Cai, Y., Xue, C., Cheng, G.P.M., Zheng, Y., Wang, Y., 2022. Measuring human corneal stromal biomechanical properties using tensile testing combined with optical coherence tomography. Front. Bioeng. Biotechnol. 10 https://doi.org/10.3389/fbioe.2022.882392.

Studer, H., Larrea, X., Riedwyl, H., Büchler, P., 2010. Biomechanical model of human cornea based on stromal microstructure. J. Biomech. https://doi.org/10.1016/j.jbiomech.2009.11.021.

Sun, W., Sacks, M.S., Scott, M.J., 2005. Effects of boundary conditions on the estimation of the planar biaxial mechanical properties of soft tissues. J. Biomech. Eng. 127, 709–715. https://doi.org/10.1115/1.1933931.

Volokh, K.Y., 2017. On arterial fiber dispersion and auxetic effect. J. Biomech. 61, 123–130. https://doi.org/10.1016/j.jbiomech.2017.07.010.

Wang, S., Hatami-Marbini, H., 2021. Constitutive modeling of corneal tissue: influence of three-dimensional collagen fiber microstructure. J. Biomech. Eng. 143, 1–9. https://doi.org/10.1115/1.4048401.

Whitford, C., Studer, H., Boote, C., Meek, K.M., Elsheikh, A., 2015. Biomechanical model of the human cornea: considering shear stiffness and regional variation of collagen anisotropy and density. J. Mech. Behav. Biomed. Mater. 42, 76–87. https://doi.org/10.1016/j.jmbbm.2014.11.006.

Winkler, M., Shoa, G., Xie, Y., Petsche, S.J., Pinsky, P.M., Juhasz, T., Brown, D.J., Jester, J.V., 2013a. Three-dimensional distribution of transverse collagen fibers in the anterior human corneal stroma. Investig. Ophthalmol. Vis. Sci. 54, 7293–7301. https://doi.org/10.1167/iovs.13-13150.

Winkler, M., Shoa, G., Xie, Y., Petsche, S.J., Pinsky, P.M., Juhasz, T., Brown, D.J., Jester, J.V., 2013b. Three-dimensional distribution of transverse collagen fibers in the anterior human corneal stroma. Investig. Ophthalmol. Vis. Sci. 54, 7293–7301. https://doi.org/10.1167/iovs.13-13150.

Xia, D., Zhang, S., Hjortdal, J.Ø., Li, Q., Thomsen, K., Chevallier, J., Besenbacher, F., Dong, M., 2014. Hydrated Human Corneal Stroma Revealed by Quantitative Dynamic Atomic Force Microscopy at Nanoscale, pp. 6873–6882.

Xiang, Y., Shen, M., Xue, C., Wu, D., Wang, Y., 2018. Tensile biomechanical properties and constitutive parameters of human corneal stroma extracted by SMILE procedure. J. Mech. Behav. Biomed. Mater. 85, 102–108. https://doi.org/10.1016/j.jmbbm.2018.05.042.

Xue, C., Xiang, Y., Shen, M., Wu, D., Wang, Y., 2018. Preliminary investigation of the mechanical anisotropy of the normal human corneal stroma. J. Ophthalmol. 2018 https://doi.org/10.1155/2018/5392041.

Xue, C., Xiang, Y., Song, Y., Shen, M., Wu, D., Wang, Y., 2021. Direct evidence of symmetry between bilateral human corneas in biomechanical properties: a comparison study with fresh corneal tissue. J. Ophthalmol. 2021 https://doi.org/10.1155/2021/8891412.